CHEM TRENDZ JOURNAL (CHJ)

Vol. 1 No. 2 (2024) 01 – 23 | ISSN: xxxx-xxxx (Media Online)

Photocatalytic Degradation of Congo Red with Sol-Gel Immobilized TiO2 Thin Layers on the Inner Surface of a Glass Tube Column

Najib Nafis [1], Hilda Sartika [2], dan Mutia Rahmi [3]*

[1-3] Department of Chemistry, Andalas University

* e-mail : njibnafis@gmail.com

ABSTRACT

The photocatalytic degradation of Congo Red in water was carried out in a reactor with a TiO_2 film immobilized on the inner wall of a glass column tube (IWGCT-TiO_2). The TiO_2 film was prepared using titanium tetra isopropoxide (TTIP) as a precursor, via a sol-gel method followed by calcination at 400 °C. The resulting TiO_2 was characterized by UV-Vis spectrometry, XRD, and SEM. The film exhibited specific UV-Vis absorption starting at 390 nm (indicative of the anatase band gap), distinct diffraction intensity at $2\theta = 25°$ (attributed to anatase), an estimated crystallite size of approximately 8.99 nm (calculated using the Scherrer equation), and good coverage on the glass substrate. The IWGCT-TiO_2 was then placed in a batch reactor system with a 22-watt black UV light as the light source and an aerator to enhance mass transfer and oxygen availability. Under UV-Vis light, the TiO_2 surface generates electrons and positive holes, initiating the degradation of organic chemicals in the surrounding solution. Investigations into the photocatalytic degradation of Congo Red revealed that the optimal performance was achieved with a TiO_2 film thickness resulting from eight coatings. The optimal degradation rate of a 50 ppm Congo Red solution showed nearly 99.0% degradation after 240 minutes of treatment. The Langmuir-Hinshelwood kinetic analysis showed a reaction rate constant (kr) of 1.311 ppm/min and an adsorption constant (K) of 0.043/ppm. The reactor efficiency evaluation indicated a quantum yield of approximately 77% over 11.5 hours of reaction time. During the 11.5-hour photocatalytic degradation of Congo Red, intermediate simple organic compounds (such as oxalic acid) were observed before complete mineralization occurred. Control experiments (with UV light but without TiO_2 and with TiO_2 but without light) conducted for all experimental settings showed no significant degradation of Congo Red.

Article Information

Received: March 22, 2024
Revised: March 29, 2024
Online: March 30, 2024

Keywords: Congo Red, Degradation, photocatalytic, Immobilization, TiO_2

1. Introduction

The development of industry worldwide, particularly the textile industry which uses various organic compounds, has been very rapid. This has consequently led to an increasing impact on environmental pollution. Pollution can alter the physical properties of water, such as turbidity, odor, temperature rise, pH, and color. The discharge of textile industry waste can damage surface and groundwater used for human needs. The disposal of liquid waste from the textile industry, containing dyes from dyeing and printing processes, can poison aquatic biota and harm the aesthetics of water bodies. It is estimated that about 10-15% of dyes are wasted during the process and released as waste.

One of the dyes widely used in the textile industry is the Azo dye group. When bodies of water are contaminated with Azo dyes, it can block sunlight from entering the water, affecting the photosynthesis process and reducing oxygen levels in the water. Azo dyes can be carcinogenic and resistant to aerobic degradation. Under anaerobic conditions, Azo dyes can be reduced to produce aromatic amines, which are carcinogenic. To minimize the negative impact of textile industry wastewater, serious efforts are needed to develop wastewater treatment methods to make the discharge more environmentally friendly.

In general, pollution from wastewater can be addressed through chemical oxidation, biological treatment, and activated carbon adsorption. Chemical oxidation cannot mineralize all organic substances and is only suitable for removing pollutants at high concentrations. Biological treatment can be conducted aerobically or anaerobically, but it requires a long time because the microorganisms used have a slow reaction rate, and controlling temperature and pH is very challenging. The activated carbon adsorption method only involves the adsorption of pollutants without decomposition, leading to new problems. Therefore, an alternative method for wastewater treatment that is more effective and efficient is needed to address wastewater issues.

Recent research has shown that advanced oxidation processes such as sonication, ionizing radiation, the combination of UV and ozone, or hydrogen peroxide with photocatalysis using TiO_2 can degrade persistent environmental pollutants. This is because these advanced oxidation systems are capable of producing strong oxidizing species, namely $\bullet OH$ radicals. The surface of titanium dioxide (TiO_2) irradiated with UV light generates hydroxyl radicals, which degrade organic compounds into harmless end products.

Titanium dioxide (TiO_2) semiconductors have been widely used as photocatalysts due to their high catalytic reactivity. This material is chemically and biologically inert, achieves complete oxidation of pollutants within a few hours, is non-toxic, does not produce polycyclic products, is inexpensive, and can oxidize pollutants at ppb levels. The photocatalytic method using TiO_2 is very promising for wastewater treatment because it offers several advantages, such as producing harmless mineral products, being easily controlled, and using sunlight as a UV light source for wastewater and drinking water treatment.

When titanium dioxide (TiO_2) is irradiated with UV light at wavelengths (λ) ≤ 415 nm, which have energy equal to or greater than its band gap energy of 3.2 eV, charge separation (photoexcitation) occurs within the TiO_2 crystal matrix. Electrons are excited to the conduction band (CB), leaving positive holes (h+) in the valence band (VB). The positive holes react with water or OH- ions to produce hydroxyl radicals (•OH). Hydroxyl radicals are highly reactive species that degrade organic molecules into CO_2, H_2O, and halide ions if the organic molecules contain halogens. The oxidation of these organic compounds is non-selective. Titanium dioxide as a photocatalyst has been proposed to address various environmental issues, and it is highly effective in eliminating microorganisms such as bacteria and viruses, controlling odors, and degrading organic pollutants such as Azo dyes.

In early research development, TiO_2 was used as a photocatalyst in suspension systems with very fine catalyst particles. The catalytic process produced is not limited by mass transfer because the diffusion distance of organic molecules to the catalyst surface is very small. However, several drawbacks have been reported when applying this method to large-scale wastewater treatment applications: expensive and time-consuming procedures are required to separate TiO_2 particles from the solution after use, and strong adsorption of dissolved organic species by TiO_2 reduces UV light penetration. Nevertheless, many researchers have now attempted to mitigate these issues by immobilizing TiO_2 on various support materials such as titanium plates, silica, and fiberglass.

This study investigates the photocatalytic degradation of Congo Red (an Azo dye) using thin films of TiO_2 immobilized on the inner walls of a glass tube. The reactor is equipped with a UV lamp (black light) in a batch reactor system. Observations were conducted to assess the effects of initial concentration, changes in electrical conductivity, pH value, and the formation of intermediate compounds correlated with the duration of Congo Red degradation under UV irradiation. The photocatalytic method using TiO_2 presents itself as a promising alternative for wastewater treatment, offering advantages such as generating harmless mineral products and being easily controllable. It holds significant potential for wastewater treatment due to its efficiency in addressing waste management issues.

2. Materials and Method

Preparation of TiO_2 Thin Films

a. Precursor Preparation

Titanium tetraisopropoxide (TTIP) will be used as the precursor for TiO_2 thin film synthesis.

b. Sol-Gel Method

TiO2 thin films will be synthesized using the sol-gel technique. This involves hydrolysis and condensation of TTIP in a controlled solution environment.

c. Film Deposition

The TiO2 sol-gel solution will be deposited onto the inner surface of a glass tube column using a spin-coating or dip-coating method.

d. Calcination

The coated glass tube column will undergo calcination at 400°C to transform the deposited gel into crystalline TiO2 thin films.

Characterization of TiO_2 Thin Films

a. UV-Vis Spectrometry

The optical properties of the TiO_2 thin films will be characterized using UV-Vis spectrometry to confirm the band gap energy and absorption characteristics.

b. X-ray Diffraction (XRD)

XRD analysis will be performed to identify the crystalline phases and structural properties of the TiO_2 thin films.

c. Scanning Electron Microscopy (SEM)

SEM imaging will be used to examine the morphology and surface topography of the TiO_2 thin films.

Photocatalytic Degradation Experiment Setup

a. Reactor Setup

A glass tube column with immobilized TiO_2 thin films will be used as the photocatalytic reactor.

b. UV Light Source

The reactor will be illuminated with a black UV light source (typically at wavelengths ≤ 415 nm) to activate the TiO_2 photocatalyst.

c. Batch Reactor System

The experimental setup will operate in a batch mode to study the degradation kinetics of Congo Red under controlled conditions.

Experimental Variables

a. Initial Congo Red Concentration

Different initial concentrations of Congo Red solution will be prepared (e.g., 20 ppm, 50 ppm, 100 ppm) to evaluate the photocatalytic efficiency.

b. pH Adjustment

The pH of the Congo Red solution will be adjusted using acid or base to investigate its influence on degradation efficiency.

c. Electrical Conductivity Monitoring

Changes in electrical conductivity of the solution will be monitored as an indicator of degradation progress.

d. Intermediate Compound Analysis

Samples will be collected at various time intervals during the degradation process to analyze the formation of intermediate compounds using analytical techniques such as HPLC or GC-MS.

3. Result

Characterization of TiO_2 Catalyst

Characterization of TiO_2 with SEM-EDX

The SEM-EDX measurements provided information on surface topography and the chemical composition of the elements constituting the catalyst surface. Prior to SEM-EDX measurement, the glass tube samples were cut into 1cm x 1cm pieces, cleaned, and coated with gold to enhance electrical conductivity. The equipment used for coating and the SEM-EDX instrumentation can be seen in the figure

Figure 1. The photo of the sample coating equipment as the preliminary treatment (a), and the SEM-EDX equipment (b)

The data and photo measurement results shown below are from measurements where the X-ray beam direction is perpendicular from the front towards the position of the TiO_2 thin film layer on the silica glass support. Therefore, the information provided originates from the X-ray coverage passing through the matrix of the TiO_2 thin film and silica glass support. Thus, the appearance of peaks correlating with the presence of titanium can be used as an indicator of the presence of TiO_2 on the silica glass support, as depicted in the image

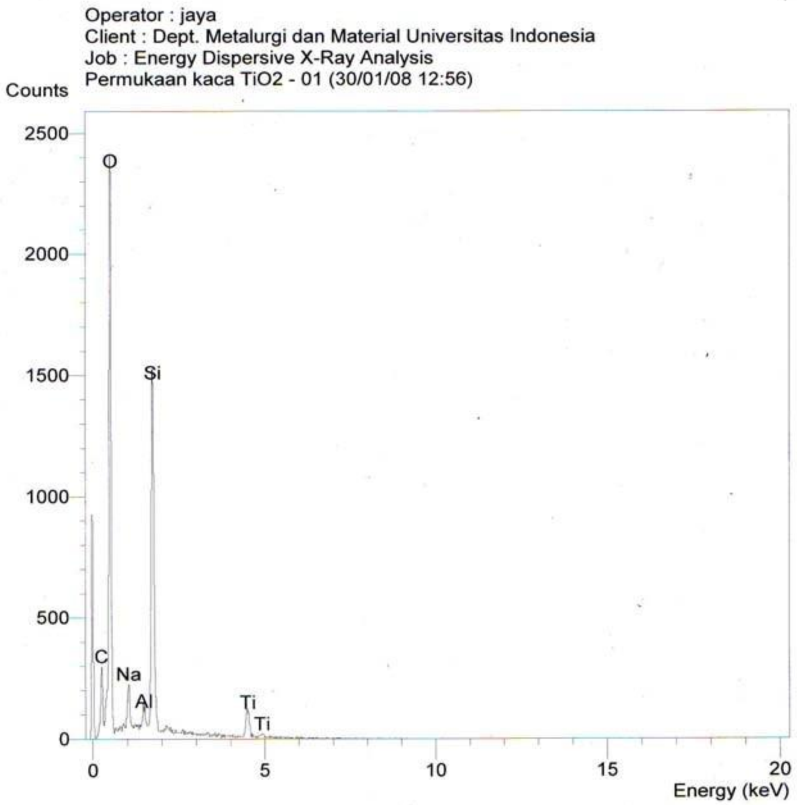

Figure 2. The measurement results of the TiO_2 thin film immobilized on the inner surface of the glass tube column using SEM-ED**.**

The SEM-EDX measurements also show the weight percentage of each constituent element inside the glass tube column that has been coated with TiO_2, as shown in the table

Tabel 1. The elemental composition within the glass tube column with TiO_2 catalyst

	Komposisi Unsur					
	C	O	Na	Al	Si	Ti
% Berat	1,51	63,73	5,95	1,48	15,36	11,97

The table above shows significant concentrations of Ti and O, which are elements composing the TiO2 thin film layer. Meanwhile, Na, Al, and Si are elements constituting the glass tube, predominantly Si indicating the presence of silicate in the glass tube.

Characterization of TiO_2 with SEM

From the SEM photo measurement results, information regarding the morphology of the TiO_2 catalyst surface can be obtained with a magnification of 1000 times, as shown in figure a. Similarly, the thickness of the TiO_2 layer can be observed at 2000 times magnification, as depicted in figure b. The images do not provide a depiction of the porosity that may exist within the TiO_2 layer matrix. However, overall, the images clearly demonstrate the presence of TiO_2 immobilized on the inner wall of the glass tube

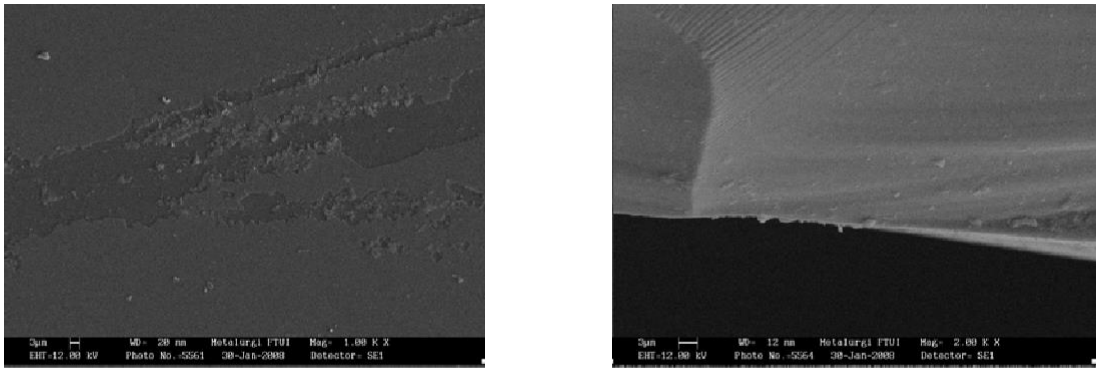

(a) (b)

Figure 3. SEM photos of the TiO2 layer surface (a) and the thickness of the TiO2 layer on the inner wall of the glass tube (b)

Characterization of TiO2 with XRD

The analysis of TiO2 crystals with XRD (X-Ray Diffraction) aims to obtain information about the crystal structure of synthesized TiO2. The TiO2 catalyst analyzed underwent calcination without being coated on a glass substrate, but received the same heat treatment as those coated on the glass substrate.

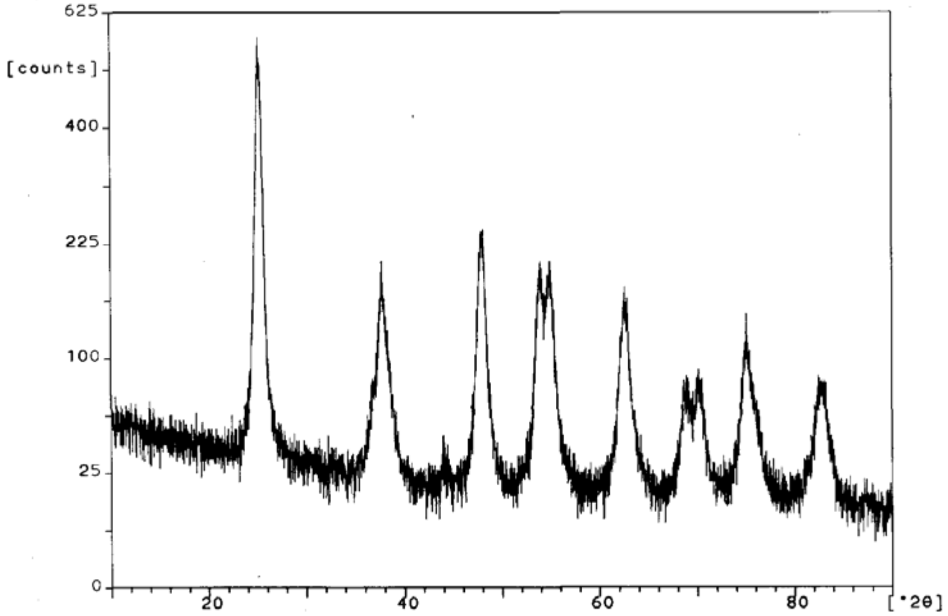

Figure 4. The results of TiO2 catalyst analysis using the sol-gel method with XRD

Figure 4 shows the X-ray diffractogram resulting from the analysis of the TiO_2 catalyst, where peaks indicate the crystal structure of TiO_2 synthesized in this study. The crystal form of TiO_2 can be determined by comparing the 2θ values or d-spacing (Å) obtained from the measurements with standard TiO_2 crystal data interpretation cards. The measured d-spacing (Å) values and interpretation data can be seen in the table

Tabel 2. The measured d-spacing (A) values and the interpretation data for TiO_2 crystal

Kartu interpretasi data d (A)		Pengukuran TiO_2 Sintesis d (A)		Keterangan
Anatase	*Rutile*	Puncak- puncak kelompok I	Puncak- puncak kelompok 2	
3,52	3,247	3,518	-	*Anatase*
2,378	2,487	2,386	-	*Anatase*
1,892	2,188	1,896	-	*Anatase*
1,699	2,054	1,697	-	*Anatase*
1,666	1,687	1,667	-	*Anatase*
1,481	1,623	1,483	-	*Anatase*
1,364	1,479	1,366	-	*Anatase*
1,338	1,359	1,340	-	*Anatase*
1,265	1,346	1,265	-	*Anatase*

The XRD measurement results of the TiO_2 catalyst show ten peaks, which, upon comparison with the data interpretation card, indicate that the synthesized TiO_2 used in this study has an anatase crystal structure. From Figure 4, using the Scherrer equation, the particle sizes of the TiO_2 produced can be calculated to be approximately 8.99 nm.

Characterization of TiO_2 with UV-Vis spectrophotometer

To obtain UV-Vis absorption characteristics, the TiO_2 thin film immobilized on the inner wall of a glass tube was examined using a UV-Vis spectrophotometer. The increase in absorption in the wavelength range between 300 – 400 nm is a characteristic feature of TiO_2 crystals, attributed to electron transitions from the valence band to the conduction band with energy gaps of 3.0 eV (rutile) and 3.2 eV (anatase). Conversely, the same glass tube without TiO_2 coating showed no absorption in this range.

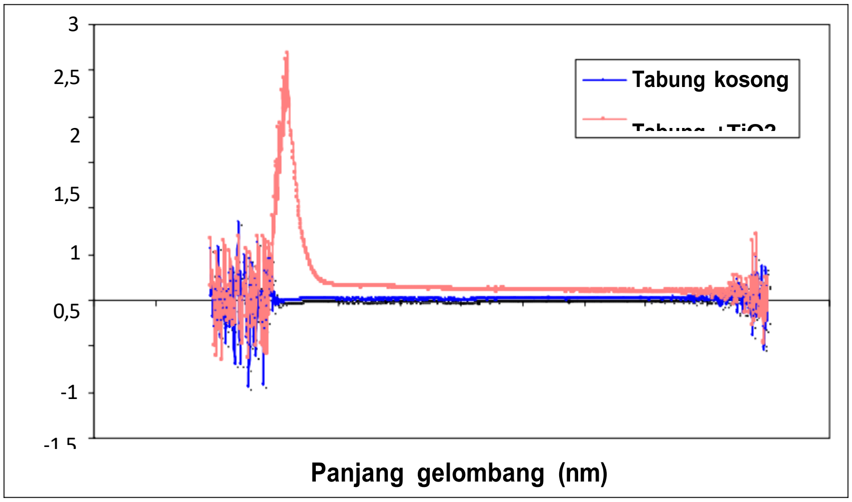

Figure 5. The absorption of the TiO_2 thin film immobilized on the inner surface of the glass tube using a UV-Vis spectrophotometer

Based on the spectrum obtained from the examination of the glass tube coated with TiO_2, an increase in absorbance occurred at a wavelength of 390 nm, equivalent to 3.2 eV, indicating the band gap energy characteristic of anatase TiO_2 crystals (conversion calculations can be seen in Appendix II). This indicates that the anatase-type TiO_2 catalyst has been well immobilized on the inner wall of the glass tube.

Gravimetric Characterization of TiO_2

In addition to using a UV-Vis spectrophotometer, TiO_2 can also be characterized gravimetrically by calculating the difference in weight between a glass tube coated with TiO_2 and a tube that is not coated with TiO_2. The TiO_2 coating adhering to the inner wall of the glass tube increases its weight in proportion to the amount of coating present. An increase in the number of coatings indicates an increase in the level of TiO_2 loading.

By converting the TiO_2 loading values based on the relationship curve between TiO_2 loading and TiO_2 layer thickness from the research conducted by Triandi, R.T and Gunlazuardi, J 38 (see Appendix IV), the TiO_2 layer thickness from this study can be determined according to the calculated TiO_2 loading as follows:

Tabel 3.

Jumlah Pelapisan	Berat Lapisan (gram)	Tingkat Pengisian TiO_2 (mg/cm^2)	Ketebalan Lapisan TiO_2 (μm)
1	0,0013	0,0119	0,0722
2	0,0025	0,0229	0,1392
3	0,0054	0,0494	0,3005
4	0,0071	0,0650	0,3955
5	0,0080	0,0732	0,4454
6	0,0097	0,0888	0,5404
7	0,0106	0,0970	0,5903
8	0,0110	0,1007	0,6128
9	0,0148	0,1354	0,8241
10	0,0154	0,1409	0,8575

Based on the data in Table 4.3, the optimal TiO_2 loading level (eight layers of TiO_2 coating) can be estimated at 0.1007 mg/cm^2, with the thickness of the TiO_2 layer adhered to the inner wall of the glass tube measuring 0.6128 μm.

Performance Test of Photocatalytic Reactor

Optimization of TiO2 Layers

To determine the optimal number of layers on the glass tube, TiO2 catalyst coating was applied multiple times on the inner wall of the glass tube. The number of TiO2 layers on the glass tube was varied from 1 to 10 times. After coating all the tubes with TiO2, they were left in an outdoor area in an inverted position for 30 minutes. This step was performed to ensure that the TiO2 layers adhered evenly to the entire inner surface of the glass tube, as shown in the figure

Figure 6. Ten glass tubes immobilized with thin layers of TiO_2

After drying, the tubes were calcined using a furnace with the temperature set initially at 150°C, then gradually increased (~4°C/minute) until reaching 400°C. Once the temperature reached 400°C, it was maintained for 1 hour to ensure the formation of anatase TiO_2 crystals proceeded effectively. It is reported that anatase TiO_2 crystals tend to be more stable at lower temperatures and exhibit higher photoactivation properties compared to other types of TiO_2 structures.

The performance of each tube with different layers of TiO2 was tested using a batch reactor system bubbled with air from an aerator to achieve optimal mass transfer. The test sample solution used was Congo Red with a volume of 10 mL and a concentration of 10 ppm for all layer variations. The decrease in Congo Red concentration was analyzed using a UV-Vis spectrophotometer, measured every 5 minutes at a wavelength of 498 nm. One of the measurement results is shown in Figure 7, indicating a decrease in absorbance over time of treatment

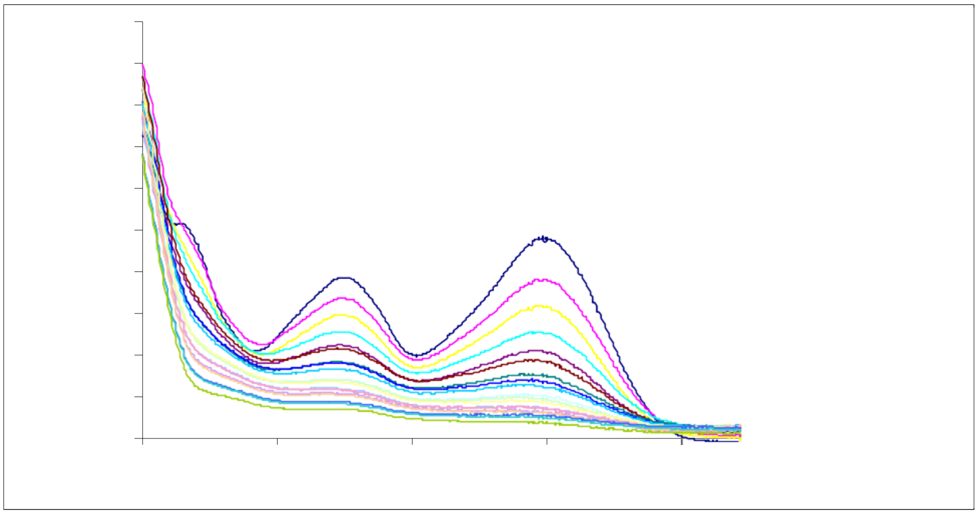

Figure 7. Absorption spectrum of Congo Red at a concentration of 10 ppm with eight layers of TiO_2

The concentration of Congo Red at each treatment time was determined using the maximum wavelength at 498 nm. The decrease in Congo Red concentration across all experimental sets with various TiO_2 layerings is shown in Figure 8. The reduction in Congo Red concentration over time was observed for several TiO_2 layering variations. The results obtained indicate that above the fifth layer on the tube, the curves overlap, suggesting similar abilities to degrade Congo Red compound

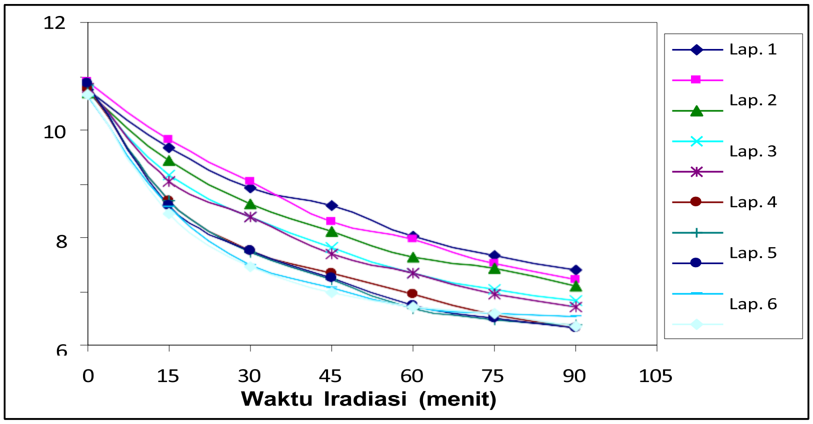

Figure 8. Graph of decreasing concentration of Congo Red per unit time for each number of TiO_2 layers

To determine the optimal number of TiO_2 layers on the glass tube for the next stage of use, it is necessary to calculate the rate constant for Congo Red degradation. The rate constant for Congo Red degradation is determined using the Langmuir-Hinshelwood (L-H) kinetic equation.

$$r = \frac{dc}{dt} = kr\theta = \frac{krKCo}{1+KCo}$$

Where dC/dt is the degradation rate of Congo Red, kr is the reaction rate constant, θ is the catalyst coverage fraction by the reactant, K is the absorption constant of the reactant, and C_o is the initial concentration of *Congo Red*.

The results of the integration of the equation above obtained the following equation :

$$\text{In} = \frac{Co}{C} + \frac{K}{1+KsCs}\,(Co - C) = \frac{krK}{1+KsCs}t$$

$$\text{In} = \frac{Co}{C} + K\,(Co - C) = krKt$$

If the initial concentration (C_o) has a very low value ($C_o \ll 1$), then the second equation will follow a first-order reaction rate equation.

$$\text{In} = \frac{Co}{Ct} = k't$$

The plot of ln C_o/Ct against irradiation time (t) produces a straight line curve with slope k'.

The relationship between the number of TiO_2 layers and the k' value representing the reaction rate that reflects the photocatalytic reactor activity is shown in Figure 9

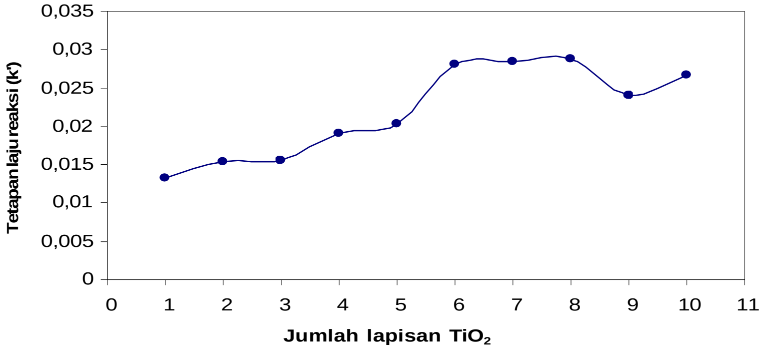

Figure 9. Optimization curve of the number of TiO_2 layers on the glass tube

From figure 9, it can be seen that the highest value of the Congo Red degradation rate constant (k') is found at eight layers of coating. Therefore, the optimal number of TiO_2 layers is eight. The degradation rate constant starts to decrease at the ninth layer. This is because the photon energy entering the surface side of the catalyst in contact with Congo Red solution begins to decrease in intensity, and there is a possibility of electron and *hole* recombination before reaching the catalyst surface. If the number of layers is too thin, not all photons hitting the TiO_2 layer surface are absorbed, resulting in fewer $^{\bullet}OH$ being formed.

Effect of Initial Concentration

To observe the effect of initial Congo Red concentration on the photocatalytic reactor activity, concentrations of 10, 20, 30, 40, 50, and 60 ppm were varied. A 10 mL Congo Red solution was placed in the optimized-coated glass tube. Each was tested in the reactor, and every 15 minutes, samples were tested with a spectrophotometer to observe absorbance reduction. Figure 10 shows the reduction in each Congo Red concentration over 150 minutes.

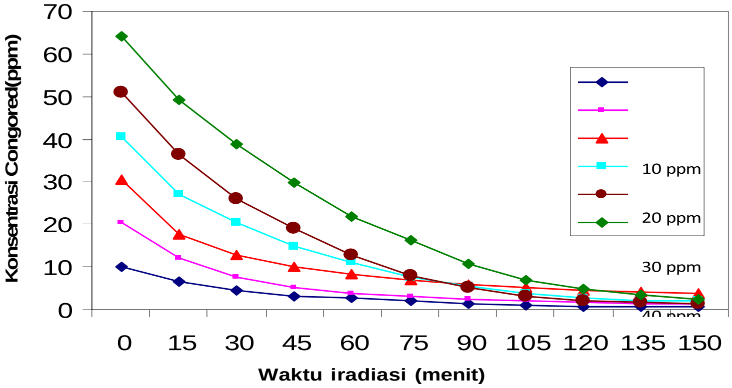

Figure 10. Graph of Congo Red concentration decrease over a 15-minute time interval

From figure 10, it can be observed that the most significant decrease in Congo Red concentration occurred at 50 ppm, where a sharp decline was evident from 0 to 30 minutes of irradiation compared to concentrations of 30, 40, and 60 ppm. The 50 ppm concentration also achieved the highest degradation value (99.0% over 240 minutes of irradiation) compared to other concentrations (data on percentage degraded and Congo Red reaction rate coefficient).

Figure 11 shows the relationship between variations in initial concentration and the degradation rate of *Congo Red*

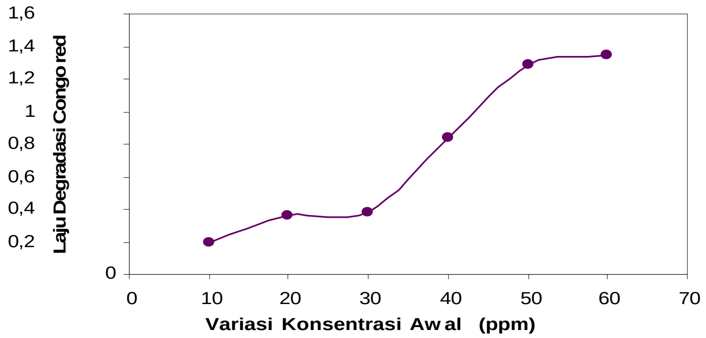

Figure 11. Relationship between initial concentration and degradation rate Congo Red

Figure 11 shows the trend of increasing degradation rate with increasing Congo Red concentration until reaching the optimum concentration where the degradation rate does not show a significant increase. The optimum concentration found in this study is 50 ppm. Meanwhile, at 60 ppm concentration, there is a slight increase in the degradation rate but it remains relatively constant. The degradation rate accelerates as the pollutant concentration increases because higher pollutant concentrations result in more adsorption onto the catalyst surface, leading to greater degradation.

The research results reported by Al Ekabi and Nick Serpone, stated that there was no longer a tendency for the degradation rate of organic pollutants to increase with increasing initial concentrations, mainly due to the saturation of the active surface coverage fraction of TiO_2. This is in accordance with the Langmuir-Hinshelwood (L-H) kinetic equation where the degree of coverage of the catalyst surface depends on the adsorption constant of organic pollutants on the catalyst surface. If the equation (L-H) is transformed into an inverse function, the following equation is obtained :

$$\frac{1}{r} = \frac{1}{kr} + \frac{1}{krKCo}$$

By plotting $1/C_o$ against $1/r$, we get a linear relationship with intercept kr^{-1} and slope (kr^{-1}, K^{-1}) as in the figure 12 :

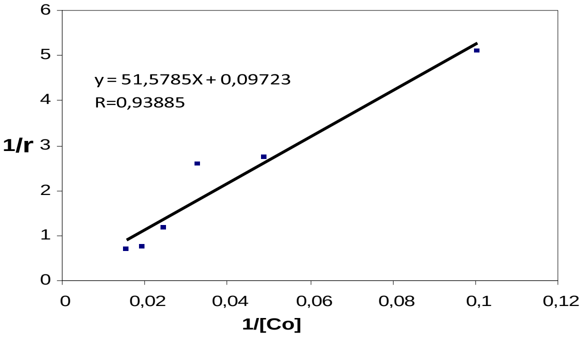

Figure 12. Correlation between the inverse reaction rate and 1/[C_o]

From figure 12, the rate constant (kr) obtained is 1.311 ppm/minute and the adsorption constant (K) is 0.043/ppm. This rate constant value provides an indication of the maximum rate achieved by the photocatalytic reactor used in this study.

Reactor Performance Test on Congo Red Degradation

To test the photocatalytic reactor's capability and demonstrate the degradation of Congo Red dye, a solution of Congo Red with a concentration of 40 ppm was prepared in 10 ml and placed in a glass tube coated with an optimal amount of TiO2 layers, then irradiated with UV light. During irradiation, samples were measured every 15 minutes using a UV-Vis spectrophotometer to monitor the decrease in absorbance of Congo Red. Congo Red exhibits absorption peaks at wavelengths of 238 nm, 344 nm, and 498 nm.

The maximum absorption in the visible light region occurs at a wavelength of 498 nm, originating from the conjugated double-bond electronic transition within the molecular structure of Congo Red. The red color observed in the solution of Congo Red molecules absorbs green light from the visible light spectrum and transmits the red component, which is complementary to the wavelength of 498 nm. Visually, the degradation of Congo Red dye is marked by the fading of the red color to colorless, as depicted in figure 13

Figure 13. The degradation results of Congo Red were irradiated with UV light with TiO_2 for 240 minutes

The degradation of Congo Red is indicated by the decrease in intensity and disappearance of its three absorption peaks due to the loss of chromophores as a result of the photocatalysis process.

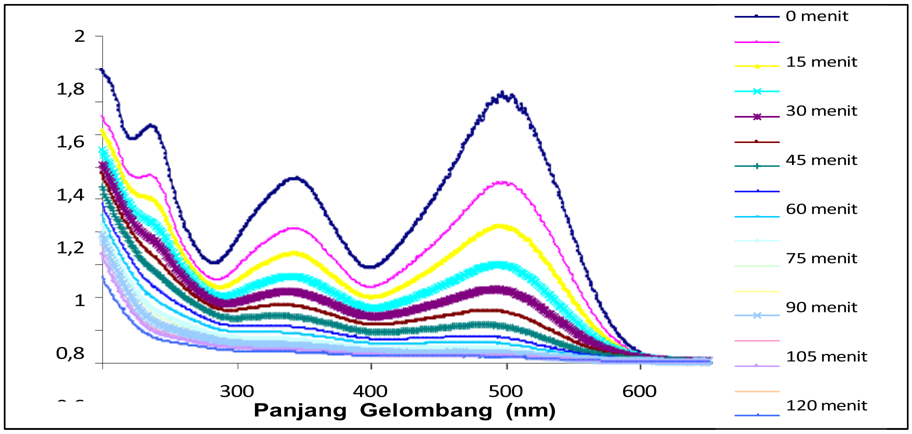

Figure 14. Absorption spectrum of Congo Red with a concentration of 40 ppm using UV light with TiO_2

From figure 14, it is evident that as the irradiation time increases, the intensity of absorption peaks at wavelengths 238 nm, 344 nm, and 498 nm decreases and eventually disappears completely. The sharp and faster decrease in intensity occurs particularly at the wavelength of 498 nm. This is because the conjugated double-bond system and its auxochromic groups are more sensitive to radiation and the photocatalytic process. The disappearance of all three peaks over the 240-minute irradiation period indicates that Congo Red has been completely degraded due to the photocatalytic reactor process.

ChatGPT To compare the photocatalytic degradation of Congo Red with its degradation via photolysis or catalysis, control experiments are necessary. These include UV irradiation without TiO2, as shown in figure 15a, and using TiO2 without UV irradiation (dark conditions), as depicted in figure 15b.

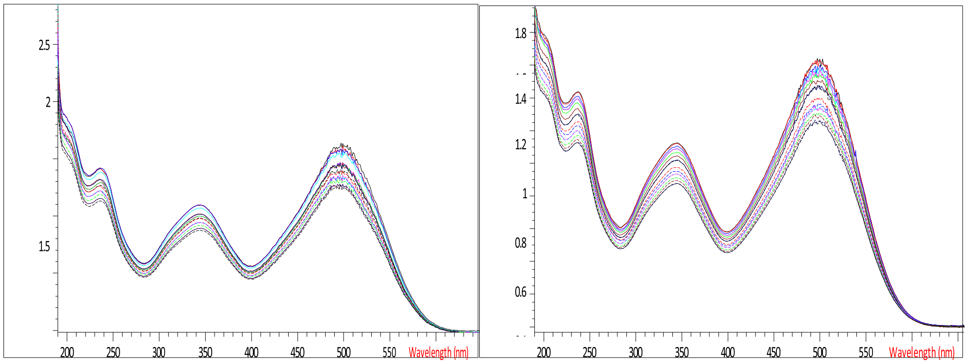

(a) (b)

Figure 15. Absorption spectrum of Congo Red concentration of 40 ppm (a) UV irradiated without TiO_2 and (b) TiO2 without UV light

Figure 15 shows the absorption spectrum of Congo Red solution under experiments with only UV light without catalyst presence (a) and with TiO_2 presence but without UV light (b), which overall can be interpreted as showing no significant decrease in Congo Red concentration. These control experiments indicate that photolysis (a) or catalysis (b) alone does not significantly contribute to the disappearance of Congo Red molecules, thus proving that the degradation or damage of Congo Red molecules is indeed caused by the photocatalysis process.

Determination of Intermediate Compounds

To study the potential formation of intermediate compounds during the degradation of Congo Red dye in the photocatalytic process, measurements were conducted on the solution before, during, and after photocatalysis. The parameters measured include :

1. Concentration of Congo Red, using spectrophotometric methods.
2. pH measurement.
3. Electrical conductivity measurement (EC).
4. Presence of intermediate compounds from Congo Red degradation, using HPLC (High Performance Liquid Chromatography).

Measurement of Congo Red Degradation Concentration Results

The decrease in concentration of Congo Red degradation products in the photocatalytic process and control experiments, namely UV irradiation without TiO_2 (photolysis) and TiO_2 without UV light (catalysis), was observed using a Congo Red solution at a concentration of 40 ppm with a volume of 10 mL. The experiments were conducted in a batch photocatalytic reactor system bubbled with air from an aerator, and the results are shown in figure 16

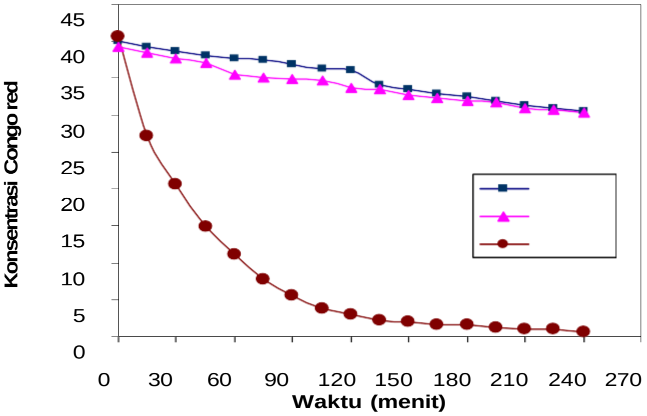

Figure 16. Graph of decreasing concentration of Congo Red degradation results

From figure 16, it is shown that in the control experiments TiO_2 without UV irradiation and UV light without TiO_2 the decrease in concentration is relatively minimal. However, in the UV irradiation process with TiO_2, there is a significant decrease in concentration from 40 ppm to 0.5 ppm after 240 minutes of irradiation. The sharp decrease in concentration in the initial minutes of irradiation is due to the diffusion process, where molecules move from areas of high concentration to low concentration. When the concentration is high, a large number of reactant molecules are absorbed on the catalyst surface, accelerating the degradation process of Congo Red.

Figure 17 depicts the graph showing the relationship between the percentage of Congo Red degraded over time. It is observed that the percentage degradation of Congo Red using TiO_2 catalyst without UV light is only 23.55%. This indicates that without UV illumination, the TiO_2 catalyst is inactive and does not generate oxidizing species (hydroxyl radicals, OH) that can degrade Congo Red molecules. However, the TiO_2 surface has the ability to absorb Congo Red, causing some Congo Red to disappear from the solution.

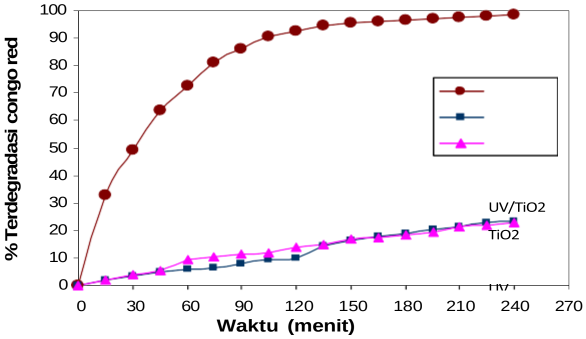

Figure 17. Graph of % Degradation of Congo Red against time (Co: 40 ppm 15 minute time variation)

In the process irradiated with UV light without TiO_2 catalyst, the percentage removal of Congo Red is only 22.78%. This indicates that photons from the UV lamp used are not effective in degrading Congo Red compounds.

In the photocatalytic process, the percentage decrease of Congo Red is 97.91% (calculation data of degraded %). This proves that the photon energy from the UV lamp hitting the TiO_2 catalyst surface causes electrons to be excited from the valence band to the conduction band, leaving holes in the valence band. Electrons in the conduction band react with oxygen molecules to form superoxide ions ($O_2^\bullet$) which subsequently form highly reactive hydroxyl radicals ($^\bullet OH$). These radicals effectively attack Congo Red compounds, leading to complete degradation

pH Value Measurement

Using the same experimental setup as described earlier, the pH value of the solution was measured at regular intervals during the process. The measurement results of the solution pH can be seen in figure 18

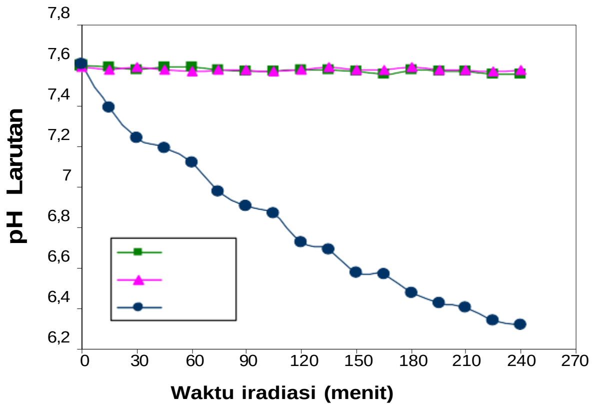

Figure 18. Changes in pH of the solution during irradiation of the Congo Red solution

The figure indicates that in the reactor system irradiated with UV light without TiO_2, the initial pH of the solution was 7.60, and in the system using TiO_2 without UV irradiation, the initial pH was 7.59. After observation for 240 minutes, there was no change in the pH of the solution. However, in the reactor system irradiated with UV light using TiO_2, the initial pH of 7.59 decreased to 6.32 after irradiation for 240 minutes. This decrease in pH is due to the formation of acidic compounds from the photodegradation reaction of Congo Red. This is consistent with previous research reported by Lachheb et al. which indicated that the pH of the solution containing Azo dye degraded by photocatalytic reaction tends to decrease (become more acidic).

The possible oxidation reaction of Congo Red molecules can be observed in the following reaction (1) :

$$C_{32}H_{22}N_6O_6S_2{}^{2-} + {}^{91}/_{2}\, O_2 \circledcirc 32CO_2 + 6NO_3{}^{-} + 2SO_4{}^{2-} + 8H^{+} + 7H_2O \quad (1)$$

From reaction (1), it can be observed that for every molecule of Congo Red that undergoes complete degradation, eight protons (H+) are produced, which will lower the pH of the solution. Tanaka et al. reported that during the degradation reactions of *Orange G and Acid Yellow 17* dyes, the simultaneous formation of sulfate ions and ammonium ions occurs, leading to an initial decrease in pH followed by stabilization at a constant pH. Another possible reaction occurring in the solution is the proton binding reaction, particularly from the degradation of amino groups, which increases the formation of ammonia as ammonium ions, as shown in reactions (2) & (3) below :

$$R - NH_2 + {}^{\bullet}H \longrightarrow {}^{\bullet}R + NH_3 \qquad (2)$$

$$NH_3 + H^{+} \longrightarrow NH_4{}^{+} \qquad (3)$$

ChatGPT In reactions (2) & (3), it explains the formation of ammonium ions ($NH_4{}^{+}$) through the attack of hydrogen radical atoms (•H) on the nitrogen atoms in the amino groups.

Hydrogen radical atoms can be generated by redox reaction (4), proton photoreduction reaction (5), or by organic acid reaction with a hole (6) as shown in the reactions below :

$$SO_3^{\bullet -} + OH^- \longrightarrow SO_4^{2-} + {}^{\bullet}H \quad (4)$$

$$H^+ + e^- \longrightarrow {}^{\bullet}H \quad (5)$$

$$H-COOH + h^+ \longrightarrow H^+ + CO_2 + {}^{\bullet}H \quad (6)$$

For Azo dyes, the reduction process can occur in two stages, leading to the cleavage of the double bond (–N=N–) into nitrogen molecules, as in reactions (7) and (8).

$$R-N=N-R' + {}^{\bullet}H \longrightarrow R-N=N^{\bullet} + R'-H \quad (7)$$

$$R-N=N^{\bullet} \longrightarrow {}^{\bullet}R + N\equiv N \quad (8)$$

Meanwhile, nitrogen in the amino groups can spontaneously form NH_4^+ ions, and then slowly oxidize to form nitrate ions.

Measuring the Value of Electrical Conductivity

Electrical conductivity (EC) in water serves as an indicator of the presence of dissolved ions originating from inorganic salts and/or soluble minerals. Soluble organic substances such as fats, oils, and alcohols cannot conduct electricity because these compounds do not dissociate into ions in water. The concept of electrical conductivity (or conductivity) of a solution refers to its ability to conduct electric current, which occurs due to the presence of dissolved anions and cations such as chloride, calcium, sodium, sulfate, and nitrate. Therefore, the electrical conductivity of a solution depends on the concentration of dissolved ions.

The analysis of electrical conductivity of the solution during Congo Red degradation was conducted on a Congo Red solution with a concentration of 40 ppm, under the conditions described in the previous subsection. The observed results can be seen in figure 19

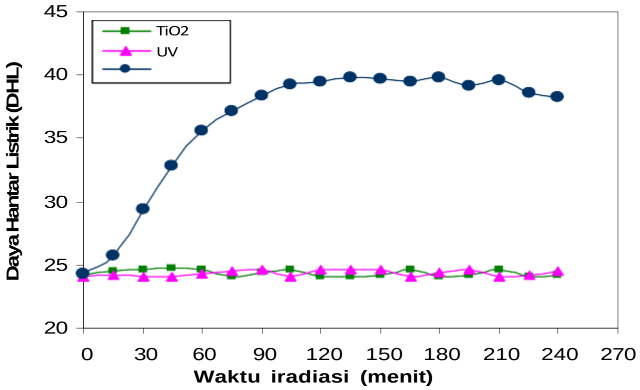

Figure 19. Value of the electrical conductivity of the solution during irradiation of the Congo Red solution

From figure 19, it can be observed that in the reactor systems with TiO_2 without UV irradiation and UV irradiation without TiO_2 during the degradation process, there was no increase in EC (Electrical Conductivity). However, in the reactor system using TiO_2 irradiated with UV for 240 minutes, there was a significant increase in EC. This increase in

EC indicates that during the photocatalytic process, ions resulting from the degradation of Congo Red molecules are formed. Specifically, for every Congo Red molecule oxidized completely, it produces 6 moles of nitrate ions (NO_3^-) and 2 moles of sulfate ions (SO_4^{2-}), along with 8 protons (H^+) as described in reaction (1).

Quantum Yield

Assuming the UV light used corresponds to a wavelength of λ = 365 nm and the black light UV lamp used has an average total absorbed intensity of 232 μW/cm^2, the quantum yield value of the photocatalytic process can be determined. The quantum yield (Φ) for the photodegradation of Congo Red is 77%. The quantum yield value increases with increasing initial concentration up to a certain point, beyond which it stabilizes. The plateauing of the quantum yield value indicates the optimum efficiency of the photocatalytic reactor used in this experiment.

4. Conclusions

Based on the research results, the following conclusions can be drawn:

a. The characterization of TiO2 catalyst immobilized on the inner wall of the glass tube using XRD revealed crystalline structure with anatase phase and TiO2 particle size of approximately 8.99 nm.
b. Optimization tests of the reactor yielded an optimum number of eight layers of TiO2, with a rate coefficient, k', of 0.02884/minute.
c. The degradation rate of Congo Red increases with higher initial concentrations, reaching an optimum concentration at 50 ppm where the degradation rate tends to plateau, achieving a degradation percentage of 99.0%.
d. Congo Red degradation is evidenced by a decrease in Congo Red concentration, pH reduction, increase in electrical conductivity, and formation of oxalic acid as an intermediate compound.
e. Oxalic acid is identified as an intermediate compound from Congo Red degradation, detected using HPLC, and undergoes further degradation as indicated by a decrease in oxalic acid concentration during 11.5 hours of irradiation.
f. The degradation rate constant of Congo Red obtained is kr = 1.311 ppm/minute, and the adsorption constant is K = 0.043/ppm, while the efficiency of the photocatalytic reactor obtained from the quantum yield value is 77%.

References

1. Sugiarto, Dasar-dasar pengolahan Air Limbah, UI Press, Jakarta, (1987).
2. Weavers, L.K., N. Malmstadt, and M.R. Hoffmann, Kinetics and Mechanism of Pentachlorophenol of Degradation by Sonication, Ozonation, and Sonolytic Ozonation, Environ. Sci. Technol. 34, (2000),1280-1285.
3. Ruppert, G., and R. Bauer, UV-O3, UV-H2O2, UV-TiO2 and The Photo- fenton Reaction Comparison of advanced Oxidation Processes for Waste Water Treatment, Chemosphere, 28 (8), (1994),1447- 1454.
4. Wu. J, Xingwang F, Yongke H, Jun L, Oxidative Decomposition of Pentacholophenol in Aqueus Solution, Radiat. Phys. Chem.,54 (4), (1998), 411-415.
5. Getoff, N., Radiation-induced Degradation of Water Pollutans-state of Art, Radiat. Phys. Chem., 47 (4), (1996), 581-593.
6. Fujishima, A. dan Honda, K., Electrochemical Photolysis of Water at Semiconductor Electrode, Nature, 238, (7), (1972), 37-38.
7. Mills, A., Davies, R.H., dan Worsley, D., Water Purification Semiconductor Photocatalysis, Chem.Soc.Rev., (1993), 417-425.
8. Dingwang, C., Fengmei, L., & Ray. A.K.,External and Internal Mass Transfer Transfer Effect on Photocatalytic Degradation, Cat. Today. 66, (2001), 475-485.
9. Linseibigler, A.L., Guangquan L., & John T.Y., Photocatalysis on TiO2 Surface : Principles, Mechanism and Selected Results, Chem. Rev., 95, (1995), 735-758.
10. Stylidi, M., Dimitris I.K., & Xenophon E.V., Pathways of Solar Ligth Induced Photocatalytic Degradation of Azo Dyes in Aqueous TiO2 Suspansions, App. Catalysis B: Environmental, 40, (2003), 271- 286.
11. Lachhep, M., Eric P., Ammar H., Mohamed K., Eliamame E., Chantal., & Jean M.H., Photocatalytic Degradation of various Type of Dyes (Alizarin S, Crocein Orange G, Methyl Red, Cango Red, Methylene Blue) in Water by UV- Irradiated Titania, App. Catalysis B: Environmental, 39, (2002), 75-90.
12. Fujishima, A., Rao, T.N, and Tryk, D.A., Titanium Dioxide Photocatalysis, Journal of Photochemistry and Photobiology C: Photochem. Rev. 1, (2000), 1-21.
13. Dijkstra, M.F.J., Buwalda, H., De Jong, A.W.F, Meliorien, A., Wilkenman, J.G.M & Beenackers, A.A.C.M., Experimental Comparison of Three Reactor Designs for Photocatalytic Water Purification, Chem. Engin. Sci., 56, (2001), 547-555.
14. Kamat, P.V., Photochemistry on Nonreactive and Reactive (Semiconductor) Surface, Chem. Rev., 93, (1993), 267-300.
15. Mills, A., & Le Hunte, S., An Overview of Semiconductor Photocatalysis, J. Photochem. Photobial.A: Chemistry, 108, (1997), 1-35.

16. Fessenden, R.J., & J.S. Fessenden, Kimia Organik, Jilid 2, Ed.3, Erlangga, Jakarta, (1986), 441-450.
17. Ismono, Cara-cara Optik Dalam Analisa Kimia, Dep. Kimia ITB, (1979), 3-14.
18. Lystyarini, A., Pengurangan Kadar Warna dengan Metode Oksidasi Fotokimia UV/H2O2, Karya Utama Sarjana Kimia FMIPA, UI, (2001)
19. Ismaningsih, Nn., Pengantar Kimia Zat Warna, Institut Teknologi Tekstil, bandung, (1979), 70-80.
20. MSDS Cango Red, Environmental Health and Savety, USA, (1999).
21. Cooper, W.J., Sunlight-induced photochemistry of humic substances in natural waters: major reactive species, (Suffet, I.H., and macCarty P, Eds.) in Aquatic humic substances, Influence of Fate and Treatment of Pollutants, Advances in Chemistry Series, American Chemical Society, Washington, DC, (1989).
22. Schwarzenbach, R.P, PM. Gschwend and D.M imboden, Environmetal Organik Chemistry, John Wiley & Son, Inc, (1993), 436-471.
23. Hoigne, J., B.C. Faust, W.R. Haag, F.E. Scully, Jr., and R.G. Zepp, Aquatic humic substances as source and sinks of photochemically produced transient reactants, (Suffet, I.H., and mcCarty, P, Eds.) in Aquatic humic substances, Influence of Fate and Treatment of Pollutants, Advances in Chemistry Series, American Chemical Society, Washington, DC, (1986)
24. Takeda,Y., Waste water treatment by ultraviolet light irradiation, UNDP/ IAEA/ RCA regional training Course on Application of Radiation Processing for Decontamination of Liquid wastes, Takasaki radiation chemistry research Establishment Jaeri, July 10-21, (1995), 100-120.
25. Sopyan, I, Fotokatalisis Semikonduktor : Teori dan terapan, Majalah BPPT Teknologi, LXXXVI, (1998).
26. Kroschwitz, J.I., Howe-Grant, M., eds., Encyclopedia of Chemical Technology, 4th ed.,Vol.18, John Wiley & Sons, New York, (1996),p. 592-593 dan 820-834.
27. Ibach, H.,& Luth, H., Solid State Physics, yang dikutip oleh Ratna, Studi Degradasi fotokatalitik Fenol dengan Katalis Suspensi TiO2 terhadap Variasi Volume dan Intensitas, Skripsi Sarjana Ilmu Kimia, FMIPA, UI, (2001).
28. Van Vlack, L.H., alih bahasa: Striati D., Ilmu dan Teknologi Bahan. Ilmu Logam dan Bukan Logam, Edisi 5, Erlangga, Jakarta, (1992), hal.161-193.
29. A. Fujishima, K., Hashimoto, T., Watanabe, TiO2 Phothocatalysts Fundamental and Applications, BKC, Inc., Japan, (1999).
30. Linsebigler, A.L, L Guangquan, and J.T. Yates. Jr. Photocatalysis on TiO2 surfaces : Principles, Mechanism, and Selected Result, Chem. Rev, 95, (1995), 735-758.

31. E. Pramauro, A.B. Prevot, M. Vincenti, G. Brizzolesi, Photocatalytic Oxidation Degradation of 4-Cholophenol in aerated Aqueus Solutions Containing TiO2 Suspension, Environ. Sci. Technol. 31, (1997), 3126-3131.
32. Miyata, T., Radiation chemistry of water systems, UNDP/ IAEA/ RCA regional Training Course on Application of Radiation Processing for Decontamination of Liquid wastes, Takasaki Radiation Chemistry Research Establishment Jaeri ,July 10-21, (1995), 70-76.
33. Hoffmann, M.R., S.T.Martin, W. Choi, and D.W. Bahnemann, Environmental Application of semiconductor photocatalysis, Chem. Rev., 95, (1995), 69-96.
34. Lizhong, S.,& Bolton, R., Determination of The Quantum Yield for The Photochemical Generation of Hydroxyl Radicals in TiO2 Suspension, J.Phys.Chem, 100, (1996), 4127-4134.
35. Serpone, N., Sauve, G., Koch, R., Tahiri, H., Pichat, P., Piccini, P., Pelizzeti, E., & Hadika, H., Standardization Protocol of Process Efficiencies and Activation Parameters in Heterogeneous Photocatalysis: Relative Photonic Efficiencies, J. Photochem. Photobiol. A: Chemistry, 94, (1996), 191-203.
36. Serpone, N., Relative Photonic Efficiencies and Quantum Yields in The Heterogeneous Photocatalysis J. Photochem. Photobiol. A: Chemistry, 104, (1997), 1-12.
37. Hedi Surahman, M. Nurdin, Yuni. K. Krisnandi, dan J. Gunlazuardi, Preparasi dan aktivitas Fotokatalitik Lapisan Tipis TiO2 yang Diimobilisasi pada Bagian Dalam Tabung Gelas Dengan Metode Sol-gel, Seminar nasional MKICS, UI, (2006), 128-133.
38. Triandi, T.R., & Gunlazuardi, J., Preparasi Lapisan Tipis TiO2 sebagai Fotokatalisis:Karakterisasi antara Ketebalan dan Aktivitas Fotokatalisis, Makara, 5, (2001), 81-91.
39. Mills, A. & Richard D., The Photomineralisation of reaktive Black 5 Sensitized by Titanium Dioxide: A study of the Initial Kinetics of Dye Photobleaching, Photocatalytic Purification and treatment Water and Air, editor: D.F.Ollis & Al-Ekabi, (1993), 595-600.
40. Subramanian, V., Prashant. V. K., & Eduardo E.W., Mass-Transfer and Kinetic Studies during the Photocatalytic Degradation of Azo Dye on Optically Transparent Elektrode Thin Film, Ind. Chem. Res.,42, (2003), 2131-2138.
41. Al-Ekabi, H. & Serpone N., Kinetic studies in Heterogeneous Photocatalysis 1. Photocatalytic Degradation of Chlorinated phenols in Aerated Aqueous Solution over TiO2 Suppoerted on a Glass Matrix, J. Phys. Chem., 92, (1988), 5726-5731.
42. Tanaka , K., Kanjana P., & Teruaki H., Photocatalytic Degradation of Comercial Azo Dyes, Wat. Res, Vol. 34, No.1, (2000), 327-333. 4
43. Spadaro, J.T., Hidroxyl Radical Mediated Degradation of Azo Dye: Evidence for Benzen Generation, Environmental Sci. And Technology, 28, (1994), 1389-1393.